Disease progression and high field MRI in CADASIL

Liem, M.K.Y.

Chapter 7

Lenticulostriate arterial lumina are normal in Cerebral Autosomal-Dominant Arteriopathy with Subcortical Infarcts and Leukoencephalopathy: A high-field in vivo MRI Study

MK Liem, J van der Grond, MJ Versluis, J Haan, AG Webb,
MD Ferrari, MA van Buchem, SAJ Lesnik Oberstein

Stroke 2010, Dec;41(12):2812-6.

ABSTRACT

Background and Purpose

Cerebral autosomal-dominant arteriopathy with subcortical infarcts and leukoencephalopathy (CADASIL) is a hereditary small vessel disease. Although postmortem studies have demonstrated mural thickening in leptomeningeal arteries and lenticulostriate perforating arteries, it is unclear whether this also leads to luminal narrowing. High-field MRI scanners enable in vivo imaging of the lumen of the lenticulostriate arteries. The aim of this study is to examine the luminal diameters of lenticulostriate arteries in living patients with CADASIL and to investigate whether luminal narrowing is correlated with the number of lacunar infarcts in the basal ganglia.

Methods

Twenty-two NOTCH3 mutation carriers and 11 healthy control subjects were examined using high-resolution 3-dimensional time-of-flight MR angiography imaging on a 7-T MRI scanner. Scans were analyzed for the presence of focal stenotic segments. The total number, length, and total cross-sectional area of lenticulostriate arteries were measured and compared between mutation carriers and control subjects. These measurements were correlated with age, disease duration, and number of lacunar infarcts in the basal ganglia.

Results

No stenotic segments were observed. No differences between mutation carriers and control subjects were found in total number of end branches (mutation carriers: mean, 14.6; control subjects: mean, 12.8), length of the lenticulostriate system, or total cross-sectional area of lenticulostriate artery lumina. Measurements of lenticulostriate artery lumina were not associated with lacunar infarct load in the basal ganglia area or with basal ganglia hyperintensities.

Conclusions

Three-dimensional time-of-flight MR angiographic on 7 T showed no differences in luminal diameters of lenticulostriate arteries between patients with CADASIL and control subjects.

INTRODUCTION

Cerebral autosomal dominant arteriopathy with subcortical infarcts and leukoencephalopathy (CADASIL) is a hereditary form of small vessel disease caused by mutations in the *NOTCH3* gene.(1) Pathological hallmarks are degeneration of vascular smooth muscle cells, deposition of granular osmiophilic material (GOM), and fibrous thickening of vessel walls.(2) It remains unclear whether stenosis, reduced cerebrovascular reactivity, or a combination of both, underlies the impaired cerebral blood flow in CADASIL.(3-6) The vessels most affected are the leptomeningeal arteries supplying the white matter, and the lenticulostriate perforating arteries supplying the deep gray nuclei.(7-9) The MRI abnormalities in these brain structures in CADASIL patients consist of white matter hyperintensities, lacunar infarcts and cerebral microbleeds.(10)

To date, vessel wall pathology could only be investigated in postmortem brain tissue. This, as well as generally low numbers of patients examined in post-mortem studies, has only given limited information about the possible haemodynamic consequences of arteriolar wall thickening in CADASIL. One study, based on 4 brain specimens, demonstrated significantly smaller luminal diameters of leptomeningeal arteries in CADASIL patients, but found only a non-significant trend to luminal narrowing in lenticulostriate penetrating arteries.(4) In living CADASIL patients, the extent of luminal narrowing has not been studied as cerebral angiography is contra-indicated in CADASIL(11) and MRI scanners at clinical field strengths (1 to 3 T) have insufficient spatial resolution to visualize these small vessels. However, recent developments in high-field (7 T and above) MRI scanners have made it possible to directly visualize the lenticulostriate perforating arteries in vivo.(12;13)

The aims of this study are to examine the luminal diameters of lenticulostriate arteries in living CADASIL patients and to investigate whether luminal narrowing of lenticulostriate arteries is correlated with the number of lacunar infarcts in the basal ganglia.

METHODS

Patients

Participants consisted of 22 symptomatic and asymptomatic NOTCH3 mutation carriers (MCs). Control subjects consisted of 11 healthy age- and sex-matched volunteers. Informed consent was obtained from all participants. Approval for the study was obtained from the institutional medical ethics committee. We took a full medical history of all participants and obtained their medical records from their physicians and general practitioners. Disease duration was determined based on first occurrence of neurological symptoms (transient ischemic attack, stroke, or cognitive decline) that could not be attributed to migraine aura.

Magnetic Resonance Imaging

MRI was performed on a whole-body human 7-T MR system (Philips Healthcare, Best, The Netherlands) equipped with a quadrature birdcage transmit and 16-channel receive array head coil (Nova Medical, Wilmington, Mass).

A 3-dimensional time-of-flight MR angiography (MRA) of the circle of Willis and lenticulostriate arteries was performed. A sagittal phase contrast localizer MRA scan was placed in the region of the basilar and carotid arteries. The volume of acquisition was then determined with a scan plane parallel to the top of the basilar artery and middle cerebral artery and with the lowest level just below the lowest point of the middle cerebral artery. The following protocol was used: 3-dimensional gradient echo images with a scan duration of 10:41 minutes per scan; repetition time/echo time/flip angle=16 ms/4.3 ms/30°, 161 slices, 180x170-mm field of view, and 784x737 matrix size resulting in a nominal resolution of 0.23x0.23x0.23 mm. A Sense factor of 3 was used to speed up the acquisition time.

To quantify basal ganglia lacunar infarct load, basal ganglia hyperintensities, and overall MRI lesion load, we also performed axial T1-, T2-, T2*-weighted scans as well as a fluid-attenuated inversion recovery scan using the following protocols: 3-dimensional T1-weighted sequence (slice thickness 0.6 mm, repetition time/echo time/flip angle 19 ms/9.2 ms/8°, matrix 700x563, field of view 210x169 mm, and scan duration of 12:08 minutes), T2-weighted spin echo sequence (slice thickness 3 mm with a 0.3 mm interslice gap, repetition time/echo time 14 000 ms/105 ms, matrix 384x288, field of view 230x184 mm, and scan duration of 6:04 minutes), 3-dimensional T2*-weighted gradient echo sequence (slice thickness 0.5 mm, repetition time/echo time/flip angle 24 ms/15 ms/15°, matrix 368x303, field of view 220x182 mm, and scan duration of 5:46 minutes), and fluid-attenuated inversion recovery sequence (slice thickness 3 mm with a 0.3-mm interslice gap, repetition time/echo time 18 832/96 ms, inversion time 2800 ms, matrix 232x168, field of view 230x184 mm, and scan duration of 5:01 minutes).

MRI Analysis

Analysis was performed on a digital workstation by 1 observer (M.K.L.) who was blinded to patient data. Postprocessing was performed using the software provided with the MRI scanner. Maximum intensity projections of the 3-dimensional time-of-flight MRA were reconstructed in the coronal (slab thickness 12 mm, overlap 11 mm, 40 slices) and axial (slab thickness 1 mm, no overlap, 38 slices) directions.

Analysis of lenticulostriate arteries

First, the coronal maximum intensity projection reconstructions were visually inspected for the possible presence of focal stenotic segments. Then we assessed the overall appearance of

the lenticulostriate system. Because the number of lenticulostriate arteries and the branching pattern per artery vary per individual, it is not feasible to select fixed arteries for diameter measurements and comparisons between individuals. Our strategy therefore was to analyze the lenticulostriate system based primarily on total number of end branches and secondarily on measures of length, diameters, and total cross-sectional area.

All visible lenticulostriate arteries originating from the middle cerebral artery, anterior cerebral artery were included in the analysis. As a primary outcome measure, the total number of end branches was counted.(13) The number of visible perforating arteries was also counted at 5 different levels: 5, 10, 15, 20, and 25 mm from the highest point of the middle cerebral artery. Arteries were considered visible if the contrast to noise ratio, compared with the surrounding brain parenchyma, was >5:1. As a secondary outcome measure, the maximum length of the lenticulostriate system was recorded by measuring the straight axial distance from the highest point of the middle cerebral artery to the end of the longest perforating artery.(12) Decreased measured length on MRA may reflect diffuse narrowing of the lenticulostriate vessels. Finally, diameters and total cross-sectional area of all visible perforating vessels were measured at the 10-mm level. Diameters were measured on the axial maximum intensity projection images using the "full-width-at-half-height" method to give the effective radius (r).(14) We used the shortest measured diameters, to avoid diameter overestimation of vessels that course non perpendicular to the sectional plane. The total cross-sectional vessel area was then calculated as $\sum(\pi r^2)$.

Analysis of lacunar infarcts, white matter hyperintensities (WMHs) and microbleeds

The MRI scans were first analyzed for overall lesion load on a digital workstation by 1 observer (M.K.L.) who was blinded to patient data. The total number of lacunar infarcts and microbleeds were counted manually. Microbleeds were defined as focal round or ovoid areas of signal loss devoid of signal hyperintensity on T1- or T2-weighted spin-echo images that show a blooming effect on T2*-weighted images.(15) Lacunar infarcts were defined as parenchymal defects not extending to the cortical gray matter with a signal intensity corresponding to that of cerebrospinal fluid on all pulse sequences, a surrounding rim of high signal intensity on the fluid-attenuated inversion recovery sequence, and a diameter >2 mm. Areas that were isointense with cerebrospinal fluid on all pulse sequences, located in the lower third of the corpus striatum of the basal ganglia, and <2 mm in diameter were excluded to differentiate lacunar infarcts from normal dilated perivascular spaces.(16) White matter hyperintensities were defined as white matter areas with increased signal intensity on T2- and fluid-attenuated inversion recovery-weighted images. Overall white matter hyperintensity load was measured using the semiquantitative Scheltens rating scale.(17)

Lesion load in the basal ganglia was analyzed separately. The number of lacunar infarcts in the basal ganglia area (including internal and external capsule) on the right and left sides

of the brain was counted manually. The amount of white matter hyperintensities in the basal ganglia region (basal ganglia hyperintensities) was measured using the basal ganglia subscale of the Scheltens rating scale.(17)

Statistics

Statistical analysis was performed using the SPSS-16 statistical software package (SPSS Inc., Chicago, IL). Because of the small sample size, especially of the control group, we used nonparametric tests for comparisons between MCs and controls and for correlation tests. The total number of end branches, number of arteries at the chosen levels, length of lenticulostriate system, and total cross-sectional area of arteries at the chosen level, were all compared between asymptomatic and symptomatic MCs and controls using Mann-Whitney *U* tests. The measurements of lenticulostriate arteries were also correlated with age and disease duration using Spearman's rank correlation coefficient (ρ). To investigate the relationship between lenticulostriate arteries and basal ganglia infarcts, we used multiple regression analysis ("enter" model) with age and lenticulostriate artery measurements as independent variables and basal ganglia infarct load and basal ganglia hyperintensity scores as the dependent variables.

RESULTS

The average age of the MCs was 45.4 years (SD, 12.1). The average age of the control subjects was 44.3 years (SD, 11.4). Twelve MCs were symptomatic with a median disease duration of 6.5 years (range, 1 to 27 years). Demographic, clinical, and overall MRI characteristics of symptomatic and asymptomatic MCs are shown in Table 1. Three patients used antihypertensive drugs: 2 symptomatic MCs used a β-blocker and 1 asymptomatic MC used an angiotensin-converting enzyme inhibitor.

Figure 1 shows an example of a coronal maximum intensity projection of the lenticulostriate arteries in a MC and control subject of similar age. Table 2 and Figure 2 show the numbers, maximum lengths, and cross-sectional areas of lenticulostriate arteries in all MCs and control subjects ordered by age and by status. No significant differences between MCs and control subjects were found neither in the primary outcome measure number of end branches nor in the secondary outcome measures length and cross-sectional area. Additional analysis for symptomatic and asymptomatic MCs separately also showed no significant differences with control subjects. Age and disease duration were not associated with any of the lenticulostriate artery measurements.

Table 1. Demographic, clinical and MRI characteristics of the study population

	MCs (n = 22)		Controls (n = 11)
	Symptomatic (n = 12)	Asymptomatic (n = 10)	
Age (mean, range)	50.6 (32-69)	39.1 (23-58)	44.3 (22-61)
Male / female	4 / 8	5 / 5	7 / 4
Hypertension	2 / 12	0 / 10	-
History of Smoking	6 / 12	3 / 10	5 / 11
Diabetes Melitus	0 / 12	0 / 10	-
Hypercholestrolemia	2 / 12	0 / 10	-
Disease Duration (years)(mean, range)	7.4 (1-27)	0	-
History of TIA/Stroke	11 / 12	0 / 10	-
Cognitive Dysfunction	2 / 12	0 / 10	-
Disability	8 / 12	0 / 10	-
Use of antihypertensive drugs	2 / 12	1 / 10	-
Overall WMH load (mean, SD)	25.5 (3.9)	17.9 (10.1)	-
Microbleeds present	6 / 12	3 / 10	-
Lacunar Infarcts present	8 / 12	3 / 10	-
Basal Ganglia Infarcts present	5 / 12	3 / 10	0 (0)
Basal Ganglia WMH load (mean, SD)	6.1 (5.0)	3.7 (5.7)	0 (0)

WMH load = White Matter Hyperintensity load (Scheltens scale)

Table 2. Lenticulostriate arteries in *NOTCH3* MCs and controls

	MCs (n = 22)	Controls (n = 11)
Total number of end branches (mean, SD)	14.6 (5.8)	12.8 (5.4)
Number of arteries at 5 mm (mean, SD)	10.2 (4.2)	9.2 (2.8)
Number of arteries at 10 mm (mean, SD)	8.0 (3.2)	7.6 (2.6)
Number of arteries at 15 mm (mean, SD)	6.0 (3.0)	6.4 (2.4)
Number of arteries at 20 mm (mean, SD)	3.0 (2.0)	3.4 (2.6)
Number of arteries at 25 mm (mean, SD)	0.6 (1.0)	1.0 (2.0)
Total cross-sectional area of arteries at 10 mm (mm^2)(mean, SD)	1.26 (0.50)	1.08 (0.42)
Length of lenticulostriate system (mm)(mean, SD)	21.9 (4.1)	22.4 (4.2)

$p > 0.05$ for all measurements

Figure 1. Coronal maximum intensity projection of a 3-dimensional time-of-flight MRA in a NOTCH3 MC (top) and a control (bottom) of similar age showing the lenticulostriate arteries (arrows) on the left side. ICA indicates internal carotid artery; ACA, anterior cerebral artery; MCA, middle cerebral artery.

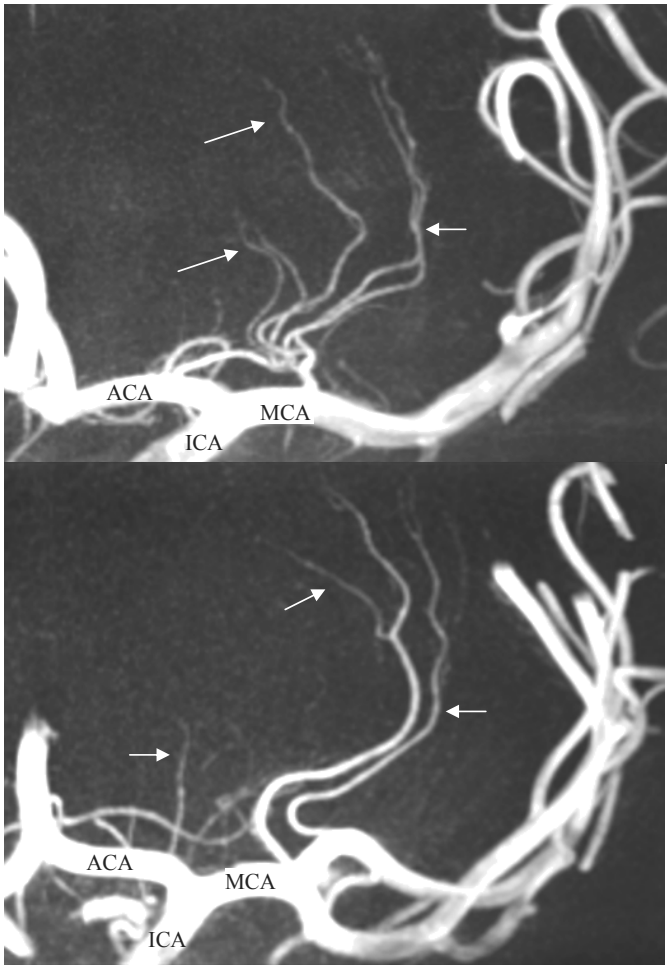

Of the 22 MCs, 11 had lacunar infarcts in the basal ganglia area (mean: 4.9, range: 1-13) and 15 had basal ganglia hyperintensities (mean Scheltens score: 5, range: 1-18). Regression analysis showed that the number, length and area of lenticulostriate arteries were not correlated with hyperintensities and lacunar infarct lesion load in the basal ganglia. The controls had no basal ganglia infarcts and no basal ganglia hyperintensities.

Figure 2. A, Total number of end branches of lenticulostriate arteries in MCs and control subjects. B, Total cross-sectional area of lenticulostriate arteries at 10 mm from their origin in MCs and control subjects. C, Length of the lenticulostriate system in MCs and control subjects.

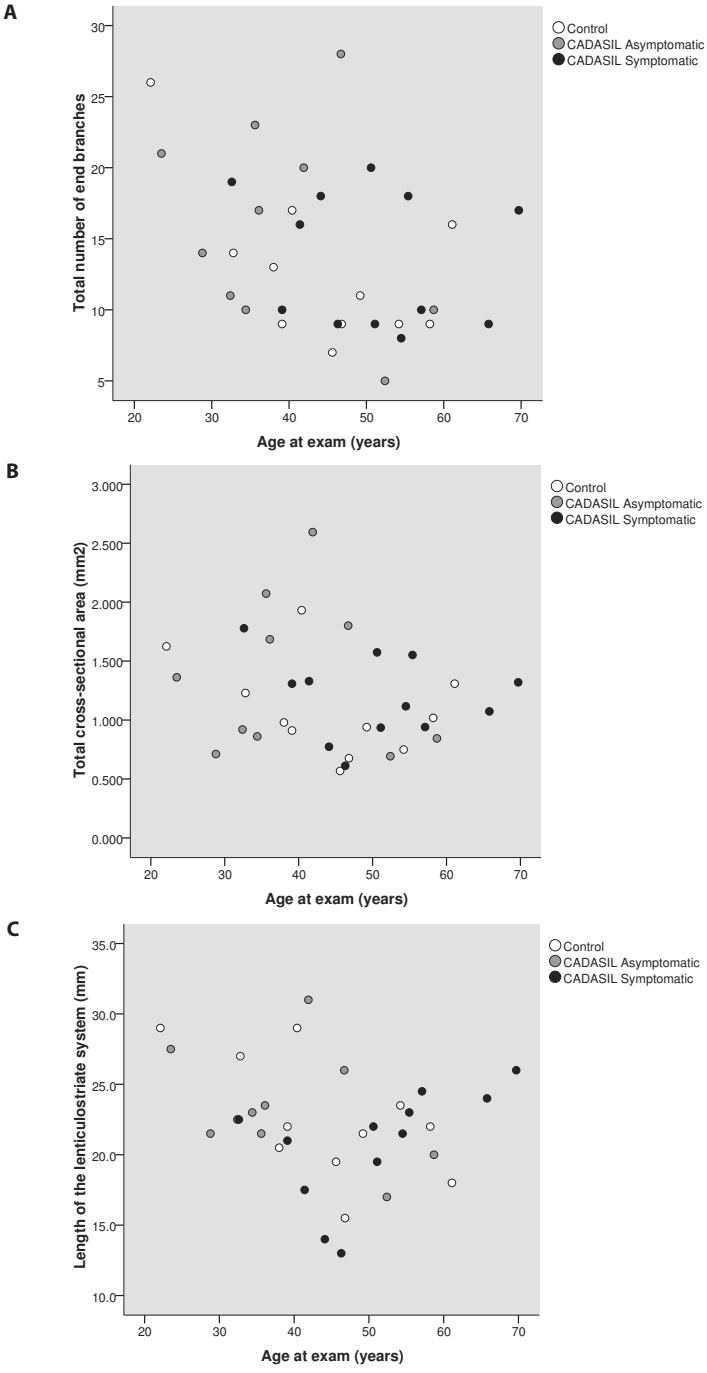

DISCUSSION

This 7-T MRA study shows that luminal diameters of lenticulostriate arteries, as indicated by measurements of length, number, and cross-sectional area, are similar in patients with CADASIL and control subjects. We found no focal stenotic segments of lenticulostriate arteries in patients with CADASIL. We also showed that luminal diameters of lenticulostriate arteries are not associated with lacunar infarct load in the basal ganglia or with basal ganglia hyperintensities.

Studies of luminal diameters in lenticulostriate arteries have not been performed before in living patients with CADASIL. Our finding that luminal diameters are normal in CADASIL seems to be in disagreement with results from postmortem studies that demonstrated wall thickening in lenticulostriate arteries.(7;8) However, our findings are in line with the suggestion from a smaller postmortem study that the neuropathological changes in the walls of lenticulostriate arteries, including thickening of the wall, may not directly lead to luminal narrowing.(4)

We found that luminal measurements were not associated with lacunar infarct load in the basal ganglia. Although basal ganglia infarcts in CADASIL are often asymptomatic, it should be noted that strategically located lacunar infarcts in the striatocapsular region can lead to sensorimotor disturbance and cognitive dysfunction.(18;19) Our findings suggest that the mechanism leading to lacunar infarcts in the basal ganglia in CADASIL is not attributable to generalized narrowing of lenticulostriate arteries, but possibly to other hemodynamic flow disturbances such as decreased cerebrovascular reactivity.(5;6) The lack of association between age and disease duration with these vascular measurements further supports the finding that generalized narrowing of luminal diameters of lenticulostriate arteries does not play a significant role in the pathophysiology of CADASIL.

Recent developments in high-field MRI have raised interest in applying these techniques to study the pathophysiology of lacunar infarcts in sporadic small vessel disease.(12) One recent 7-T MRA study demonstrated a lower number of lenticulostriate vessels in young patients with hypertension,(20) possibly caused by luminal narrowing or occlusion. Comparisons with other small-vessel diseases such as CADASIL may lead to better understanding of pathophysiologic mechanisms leading to basal ganglia infarcts. The fact that we did not find any differences in lenticulostriate arteries between patients and controls suggests that the pathophysiology of lacunar infarcts in CADASIL might be different from that of lacunar infarcts in hypertensive patients.

A limitation of this study is the spatial resolution of MRA imaging. Despite the improved resolution of high-field MRA, it is not possible to visualize vessels <250 μm with in vivo imag-

ing methods. Our conclusion that luminal diameters of lenticulostriate arteries are similar in CADASIL and control subjects is therefore based on vessels >250 µm. Luminal narrowing in smaller vessels can therefore not be ruled out.(21) However, the relative contribution of these small vessels to basal ganglia perfusion is relatively low, compared to the vessels that were imaged. A post mortem study about lenticulostriate arteries did not demonstrate luminal narrowing in CADASIL.(4)

It should be noted that the reading method used for MRA analysis has not been validated yet. Since MRA of lenticulostriate arteries is a relatively new technique, no validation studies have been performed. Validation studies are hard to perform, since measurements are highly dependable on MRI scan parameters and field strength,(22) and since the only possible in-vivo gold standard of DSA is an invasive technique. Also, the unique anatomy of the lenticulostriate system makes it impossible to use reading methods that have been applied to other vessels in other MRA studies. From our parameters, the number of end branches is an objective parameter and is therefore used as the primary outcome measure. A limitation of the parameter length is that it does not take into account tortuosity. However, it could still be considered a measurement of penetration depth into the deep gray matter. A limitation of the parameters diameters and cross-sectional area is that the measurements can be influenced by a non perpendical course of the vessel to the scanplane.

It should be realized that the signal intensity in blood vessels, as imaged by 3-dimensional time-of-flight MRA, is dependent on the rate of blood flow. Luminal diameters may be underestimated in areas of slow blood flow. However, if slow blood flow would be present in CADASIL, and it would have influenced the 3-dimensional time-of-flight measurements, it would have led to lower measured luminal diameters in patients with CADASIL. In our study we found no difference in luminal diameters, which suggests that slow blood flow is not a mitigating factor in our measurements.

Another problem is the variety in measurements found across both the group of patients with CADASIL and the control subjects. Because it also involved control subjects, it is more likely based on normal interindividual variation or on limitations of the MRI technique than on vessel pathology. However, this variety makes it harder to detect additional pathological processes and thus increases the chance of Type II error.

In conclusion, high-field MRA showed no differences in luminal diameters of lenticulostriate arteries between patients with CADASIL and control subjects, suggesting that the mechanism that leads to basal ganglia damage in CADASIL is possibly based on other mechanisms than anatomic narrowing of vessel lumina.

REFERENCE LIST

(1) Joutel A, Vahedi K, Corpechot C, Troesch A, Chabriat H, Vayssiere C, et al. Strong clustering and stereotyped nature of Notch3 mutations in CADASIL patients [see comments]. Lancet 1997; 350(9090):1511-5.

(2) Ruchoux MM, Guerouaou D, Vandenhaute B, Pruvo JP, Vermersch P, Leys D. Systemic vascular smooth muscle cell impairment in cerebral autosomal dominant arteriopathy with subcortical infarcts and leukoencephalopathy. Acta Neuropathol (Berl) 1995;89(6):500-12.

(3) Miao Q, Paloneva T, Tuominen S, Poyhonen M, Tuisku S, Viitanen M, et al. Fibrosis and stenosis of the long penetrating cerebral arteries: the cause of the white matter pathology in cerebral autosomal dominant arteriopathy with subcortical infarcts and leukoencephalopathy. Brain Pathol 2004 Oct;14(4):358-64.

(4) Miao Q, Paloneva T, Tuisku S, Roine S, Poyhonen M, Viitanen M, et al. Arterioles of the lenticular nucleus in CADASIL. Stroke 2006 Sep;37(9):2242-7.

(5) Liem MK, Lesnik Oberstein SA, Haan J, Boom R, Ferrari MD, Buchem MA, et al. Cerebrovascular reactivity is a main determinant of white matter hyperintensity progression in CADASIL. AJNR Am J Neuroradiol 2009 Jun;30(6):1244-7.

(6) Chabriat H, Pappata S, Ostergaard L, Clark CA, Pachot-Clouard M, Vahedi K, et al. Cerebral hemodynamics in CADASIL before and after acetazolamide challenge assessed with MRI bolus tracking. Stroke 2000 Aug;31(8):1904-12.

(7) Baudrimont M, Dubas F, Joutel A, Tournier-Lasserve E, Bousser MG. Autosomal dominant leukoencephalopathy and subcortical ischemic stroke. A clinicopathological study. Stroke 1993 Jan; 24(1):122-5.

(8) Jung HH, Bassetti C, Tournier-Lasserve E, Vahedi K, Arnaboldi M, Arifi VB, et al. Cerebral autosomal dominant arteriopathy with subcortical infarcts and leukoencephalopathy: a clinicopathological and genetic study of a Swiss family. J Neurol Neurosurg Psychiatry 1995;59(2):138-43.

(9) Kalimo H, Ruchoux MM, Viitanen M, Kalaria RN. CADASIL: a common form of hereditary arteriopathy causing brain infarcts and dementia. Brain Pathol 2002 Jul;12(3):371-84.

(10) van den Boom R, Lesnik Oberstein SA, Ferrari MD, Haan J, Van Buchem MA. Cerebral autosomal dominant arteriopathy with subcortical infarcts and leukoencephalopathy: MR imaging findings at different ages--3rd-6th decades. Radiology 2003 Dec;229(3):683-90.

(11) Dichgans M, Petersen D. Angiographic complications in CADASIL. Lancet 1997 Mar 15;349(9054): 776-7.

(12) Hendrikse J, Zwanenburg JJ, Visser F, Takahara T, Luijten P. Noninvasive depiction of the lenticulostriate arteries with time-of-flight MR angiography at 7.0 T. Cerebrovasc Dis 2008;26(6):624-9.

(13) Kang CK, Park CW, Han JY, Kim SH, Park CA, Kim KN, et al. Imaging and analysis of lenticulostriate arteries using 7.0-Tesla magnetic resonance angiography. Magn Reson Med 2009 Jan;61(1): 136-44.

(14) Hernandez-Hoyos M, Orkisz M, Puech P, Mansard-Desbleds C, Douek P, Magnin IE. Computer-assisted analysis of three-dimensional MR angiograms. Radiographics 2002 Mar;22(2):421-36.

(15) Greenberg SM, Vernooij MW, Cordonnier C, Viswanathan A, Al-Shahi SR, Warach S, et al. Cerebral microbleeds: a guide to detection and interpretation. Lancet Neurol 2009 Feb;8(2):165-74.

(16) Bokura H, Kobayashi S, Yamaguchi S. Distinguishing silent lacunar infarction from enlarged Virchow-Robin spaces: a magnetic resonance imaging and pathological study. J Neurol 1998 Feb; 245(2):116-22.

(17) Scheltens P, Barkhof F, Leys D, Pruvo JP, Nauta JJ, Vermersch P, et al. A semiquantative rating scale for the assessment of signal hyperintensities on magnetic resonance imaging. J Neurol Sci 1993; 114(1):7-12.

(18) Fries W, Danek A, Scheidtmann K, Hamburger C. Motor recovery following capsular stroke. Role of descending pathways from multiple motor areas. Brain 1993 Apr;116 (Pt 2):369-82.

(19) Gold G, Kovari E, Herrmann FR, Canuto A, Hof PR, Michel JP, et al. Cognitive consequences of thalamic, basal ganglia, and deep white matter lacunes in brain aging and dementia. Stroke 2005 Jun;36(6):1184-8.

(20) Kang CK, Park CA, Lee H, Kim SH, Park CW, Kim YB, et al. Hypertension correlates with lenticulostriate arteries visualized by 7T magnetic resonance angiography. Hypertension 2009 Nov;54(5): 1050-6.

(21) Joutel A, Monet-Lepretre M, Gosele C, Baron-Menguy C, Hammes A, Schmidt S, et al. Cerebrovascular dysfunction and microcirculation rarefaction precede white matter lesions in a mouse genetic model of cerebral ischemic small vessel disease. J Clin Invest 2010 Feb 1;120(2):433-45.

(22) Al-Kwifi O, Emery DJ, Wilman AH. Vessel contrast at three Tesla in time-of-flight magnetic resonance angiography of the intracranial and carotid arteries. Magn Reson Imaging 2002 Feb;20(2): 181-7.